

Sequence-Specific Assignment of Ligand Cysteine Protons of Oxidized, Recombinant HiPIP I from *Ectothiorhodospira halophila*

Ivano Bertini,^{*,†} Francesco Capozzi,[‡] Lindsay D. Eltis,[§] Isabella Caterina Felli,[†] Claudio Luchinat,[‡] and Mario Piccioli[†]

Department of Chemistry, University of Florence, Via Gino Capponi 7, 50121 Florence, Italy, Institute of Agricultural Chemistry, Viale Berti Pichat 10, 40127 Bologna, Italy, and Department of Biochemistry, Université Laval, Québec City, Québec, G1K 7P4, Canada

Received January 6, 1995[®]

The ¹H NMR spectra of the oxidized high-potential iron–sulfur protein (HiPIP) I from *Ectothiorhodospira halophila* have been investigated, and the sequence-specific assignment of the protons of the cluster-bound cysteines has been performed. The spectrum of this protein is different from those of the six other proteins investigated to date in that at least one hyperfine shifted signal is missing. It is demonstrated that the “missing” signals of the βCH₂ protons of Cys 66 are under the diamagnetic envelope at 2.60 and 6.30 ppm (at 288 K). The hyperfine shifts of these protons and those of the βCH₂ protons of Cys 36 are consistent with the proposition that the oxidized cluster is in equilibrium between two electronic species. These species differ with respect to their valence distribution within the protein frame and are present in a molar ratio of about 4:1 at room temperature. An empirical relationship between the hyperfine shifts of the βCH₂ protons of Cys 36 and 66 and the percentage of the two electronic species is proposed.

Introduction

High-potential iron–sulfur proteins from photosynthetic bacteria (HiPIPs hereafter) are a class of intensively investigated proteins.^{1–8} The valence distribution within the four-iron cluster of oxidized HiPIPs is not well understood and may be relevant to elucidating the factors determining the redox potential. The cluster contains two iron(III) ions and a mixed-valence pair in which the iron ions have oxidation number +2.5.^{9,10} The cluster of HiPIP II from *E. halophila* is the best understood system: its ESR spectrum at 4 K is consistent with an *S* = 1/2 ground state,¹¹ and magnetic Mössbauer data indicate that this *S* = 1/2 state is the result of antiferromagnetic coupling between the mixed-valence pair and the iron(III) pair, the former having a larger subspin than the latter.^{12,13} This arises because the

hyperfine coupling with ⁵⁷Fe of Fe^{2.5+} has a regular sign while that of Fe³⁺ has a reversed sign, indicative of negative and positive (*S_z*) for the Fe^{2.5+} pair and the Fe³⁺ pair, respectively. This interpretation of the electronic structure of the oxidized cluster of HiPIP II from *E. halophila*, which is also valid for model compounds,^{14,15} is consistent with NMR data. The NMR spectrum of this protein possesses two clearly divided sets of four signals arising from cysteine βCH₂ proton signals, one set being upfield and the other, downfield¹⁶ (Figure 1B). This spectrum has been interpreted by assigning a negative (*S_z*) to the mixed-valence pair, thus accounting for the downfield hyperfine shifts of the βCH₂ protons of the cysteines ligated to this pair of ions, and a positive (*S_z*) to the ferric pair, accounting for the upfield hyperfine shifts of the βCH₂ protons of the cysteines ligated to the ferric pair.^{17,18} With increasing temperature, the upfield shifted signals move rapidly toward the diamagnetic region of the spectrum, and at infinite temperature, their shifts extrapolate to far downfield. This behavior, which we termed pseudo-Curie,¹⁹ is observed because the excited states of the ferric ions, which increase in population, have negative (*S_z*). Our sequence-specific assignment of the cysteines bound to each kind of iron ion¹⁸ indicates that the oxidized cluster of *E. halophila* HiPIP II is represented by the left-hand side of the equilibrium shown in Figure 1A.

In all other characterized HiPIPs, only one of the two cysteines bound to the ferric ions has upfield-shifted βCH₂ protons, while the βCH₂ protons of the other cysteine are

[†] University of Florence.

[‡] Institute of Agricultural Chemistry.

[§] Université Laval.

[®] Abstract published in *Advance ACS Abstracts*, April 1, 1995.

- (1) Adman, E. T.; Sieker, L. C.; Jensen, L. H. *J. Biol. Chem.* **1976**, *251*, 3801.
- (2) Benning, M. M.; Meyer, T. E.; Rayment, I.; Holden, H. M. *Biochemistry* **1994**, *33*, 2476–2483.
- (3) Langen, R.; Jensen, G. M.; Jacob, U.; Stephen, P. J.; Warshel, A. J. *Biol. Chem.* **1992**, *267*, 25625–25627.
- (4) Carter, C. W. J.; Kraut, J.; Freer, S. T.; Xuong, N.-H.; Alden, R. A.; Bartsch, R. G. *J. Biol. Chem.* **1974**, *249*, 4212–4215.
- (5) Breiter, D. R.; Meyer, T. E.; Rayment, I.; Holden, H. M. *J. Biol. Chem.* **1991**, *266*, 18660–18667.
- (6) Przysiecki, C. T.; Meyer, T. E.; Cusanovich, M. A. *Biochemistry* **1985**, *24*, 2542–2549.
- (7) Backes, G.; Mino, Y.; Loehr, T. M.; Meyer, T. E.; Cusanovich, M. A.; Sweeney, W. V.; Adman, E. T.; Sanders-Loehr, J. *J. Am. Chem. Soc.* **1991**, *113*, 2055–2064.
- (8) Huang, J.; Ostrander, R. L.; Rheingold, A. L.; Leung, Y.; Walters, M. A. *J. Am. Chem. Soc.* **1994**, *116*, 6769–6776.
- (9) Middleton, P.; Dickson, D. P. E.; Johnson, C. E.; Rush, J. D. *Eur. J. Biochem.* **1980**, *104*, 289–296.
- (10) Bertini, I.; Campos, A. P.; Luchinat, C.; Teixeira, M. *J. Inorg. Biochem.* **1993**, *52*, 227–234.
- (11) Beinert, H.; Thomson, A. J. *Arch. Biochem. Biophys.* **1983**, *222*, 333–361.
- (12) Moss, T. H.; Bearden, A. J.; Bartsch, R. G.; Cusanovich, M. A. *Biochemistry* **1968**, *7*, 1591–1596.

- (13) Dickson, D. P. E.; Johnson, C. E.; Cammack, R.; Evans, M. C. W.; Hall, D. O.; Rao, K. K. *Biochem. J.* **1974**, *139*, 105.
- (14) Mouesca, J. M.; Rius, G. J.; Lamotte, B. *J. Am. Chem. Soc.* **1993**, *115*, 4714–4731.
- (15) Gloux, J.; Gloux, P.; Lamotte, B.; Mouesca, J. M.; Rius, G. J. *J. Am. Chem. Soc.* **1994**, *116*, 1953–1961.
- (16) Krishnamoorthi, R.; Markley, J. L.; Cusanovich, M. A.; Przysiecki, C. T.; Meyer, T. E. *Biochemistry* **1986**, *25*, 60–67.
- (17) Banci, L.; Bertini, I.; Briganti, F.; Luchinat, C.; Scozzafava, A.; Vicens Oliver, M. *Inorg. Chim. Acta* **1991**, *180*, 171–175.
- (18) Banci, L.; Bertini, I.; Capozzi, F.; Carloni, P.; Ciurli, S.; Luchinat, C.; Piccioli, M. *J. Am. Chem. Soc.* **1993**, *115*, 3431–3440.
- (19) Bertini, I.; Briganti, F.; Luchinat, C.; Scozzafava, A.; Sola, M. *J. Am. Chem. Soc.* **1991**, *113*, 1237–1245.

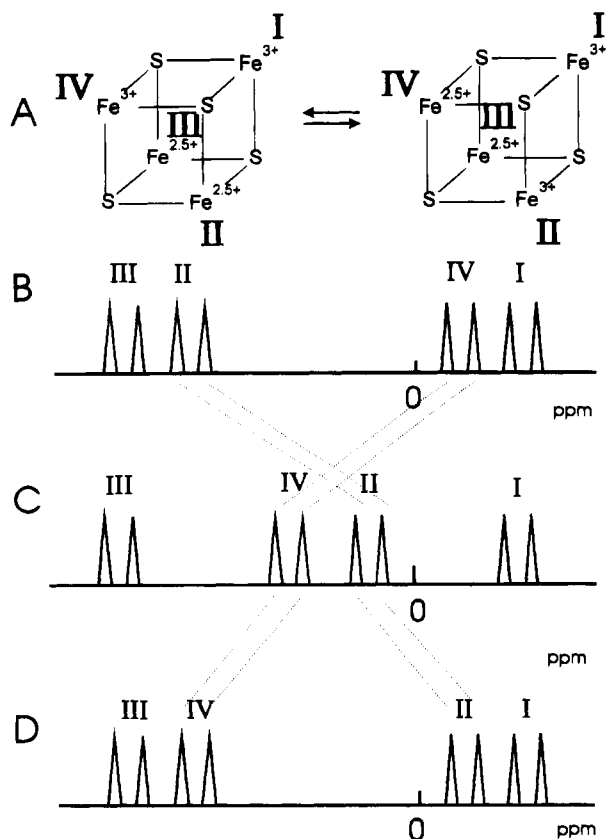


Figure 1. (A) Schematic representation of the equilibrium between two electronic distributions in HiPIP clusters. (B–D) Schematic representations of the ^1H NMR spectra of oxidized HiPIPs for various valence distributions within the cluster: (B) limiting situation in which Cys I and IV are bound to the purely ferric iron ions and Cys III and II, to the mixed-valence iron ions; (D) limiting situation in which Cys I and II are bound to the purely ferric iron ions and Cys III and IV, to the mixed-valence pair; (C) intermediate situation in which the system is in chemical equilibrium between the valence distribution of cases B and D. The situation depicted in case C is that of an equilibrium in which the molar ratio between state B and state D is about 40:60. Cysteines are numbered according to their relative positions in the linear amino acid sequence.

downfield shifted, albeit to a lesser extent than those of the cysteines bound to the irons of mixed valence.^{18–22} The temperature dependence of the latter pair of signals is of anti-Curie type (*i.e.*, the shifts increase with increasing temperature). The signals of both pairs extrapolate far downfield at infinite temperature. These data have been interpreted by assuming the existence of an equilibrium between two electronic distributions in the cluster; both distributions have mixed-valence and ferric pairs, but one iron ion that is mixed valence in one distribution becomes ferric in the other and vice versa (Figure 1A).²³ This equilibrium is fast on the NMR time scale. According to this interpretation, the ferric ion which exists transiently in the mixed-valence state induces a small downfield shift on the cysteine proton signals (Figure 1). Conversely, the $\text{Fe}^{2.5+}$ ion which exists transiently in the Fe^{3+} state induces a downfield shift which, while still sizable, is smaller than that induced by the 100% $\text{Fe}^{2.5+}$ ion (Figure 1C).

We report here the NMR spectrum of the oxidized HiPIP I from *E. halophila*. This spectrum is unique in that a hyperfine shifted signal is “missing” with respect to the pattern reported in Figure 1.¹⁶ A more intensive investigation of this system demonstrated that the spectrum of this protein is nevertheless fully consistent with the existence of an equilibrium between two electronic distributions within the cluster. Furthermore, the data enable the formulation of an empirical relationship between the hyperfine shifts and the percentage of each electronic distribution of the cluster.

Experimental Section

Recombinant HiPIP I from *E. halophila* was obtained as described previously.²⁴ Protein solutions in H_2O and D_2O were prepared at pH 5.1, in 50 mM phosphate buffer. In order to maintain the protein in the fully oxidized state, a buffered solution (50 mM phosphate buffer, pH 5.1) of $[\text{Fe}(\text{CN})_6]^{3-}$ was added to the sample, up to a final concentration of about 1.0 mM.

All NMR spectra were recorded at 288 or 298 K on a Bruker AMX 600 spectrometer, operating at a magnetic field of 14.1 T. Two-dimensional NOESY²⁵ and clean-TOCSY²⁶ experiments were performed using a spectral window of 8650 Hz. In the NOESY experiments, mixing times of 15 and 100 ms and recycle delays of 0.85–1.2 s were used. Between 750 and 950 increments were collected over 4096 data points in the acquisition dimension. In some experiments, a 2.5 ms trim pulse was applied prior to the beginning of the sequence. An additional NOESY experiment was performed to detect connectivities involving hyperfine shifted signals.²⁷ A 1024×356 data point matrix was collected over a spectral window of 85 kHz in both dimensions. Mixing and recycle delays were 9 ms and 62 ms, respectively. In order to reduce the spectral window as much as possible, the carrier frequency was placed at 36.3 ppm, and water presaturation was accomplished using an off-resonance DANTE sequence.²⁸ In the clean-TOCSY experiments, spin lock and recycle delays of 45 ms and 1.3 s, respectively, were used. The delay used between the pulses of the clean TOCSY MLEV-17 sequence was 2.0–2.2 times the 90° pulse at the chosen spin lock field. The strength of the spin lock field was 10 kHz. Between 915 and 980 increments were collected using 4096 data points. A second clean-TOCSY experiment was recorded with spin lock and recycle delays of 15 ms and 500 ms, respectively. In all two-dimensional experiments, the strong water signal was suppressed by presaturation of the solvent signal during the relaxation delay and, in the NOESY experiment, again during the mixing time. The 2D experiments were recorded using either the TPPI mode²⁹ or the States-TPPI mode.³⁰ Raw data were processed using a cosine squared filter function in both dimensions. A polynomial baseline correction was applied in both dimensions. Data were always zero-filled in order to obtain $2\text{K} \times 2\text{K}$ data point matrices. Chemical shift values were calibrated by assigning to the water signal shift values of 4.93 and 4.81 ppm from DSS at temperatures of 288 and 298 K, respectively.

1D NOE experiments on the hyperfine shifted signals were performed using the superWEFT pulse sequence ($\text{RD}-180^\circ-\tau-90^\circ-\text{AQ}$).³¹ Selective irradiation of hyperfine shifted signals was accomplished during the delay τ , using a previously described procedure.³² The irradiation time was varied from 20 to 170 ms in order to

(20) Banci, L.; Bertini, I.; Briganti, F.; Luchinat, C.; Scozzafava, A.; Vicens Oliver, M. *Inorg. Chem.* **1991**, *30*, 4517–4524.

(21) Bertini, I.; Capozzi, F.; Luchinat, C.; Piccioli, M. *Eur. J. Biochem.* **1993**, *212*, 69–78.

(22) Bertini, I.; Gaudemer, A.; Luchinat, C.; Piccioli, M. *Biochemistry* **1993**, *32*, 12887–12893.

(23) Banci, L.; Bertini, I.; Ciarli, S.; Ferretti, S.; Luchinat, C.; Piccioli, M. *Biochemistry* **1993**, *32*, 9387–9397.

(24) Eltis, L. D.; Iwagami, S. G.; Smith, M. *Protein Eng.* **1994**, *7*, 1145–1150.

(25) Macura, S.; Wüthrich, K. J.; Ernst, R. R. *J. Magn. Reson.* **1982**, *47*, 351–357.

(26) Griesinger, C.; Otting, G.; Wüthrich, K. J.; Ernst, R. R. *J. Am. Chem. Soc.* **1988**, *110*, 7870–7872.

(27) Banci, L.; Bertini, I.; Luchinat, C. In *Methods in Enzymology*; James, T. L., Oppenheimer, N. J., Eds.; Academic Press, Inc.: Orlando, FL, 1994.

(28) Morris, G. A.; Freeman, R. *J. Magn. Reson.* **1978**, *29*, 433–462.

(29) Marion, D.; Wüthrich, K. *J. Biochem. Biophys. Res. Commun.* **1982**, *113*, 967.

(30) States, D. J.; Haberkorn, R. A.; Ruben, D. J. *J. Magn. Reson.* **1982**, *48*, 286–292.

(31) Inubushi, T.; Becker, E. D. *J. Magn. Reson.* **1983**, *51*, 128–133.

(32) Banci, L.; Bertini, I.; Luchinat, C.; Piccioli, M.; Scozzafava, A.; Turano, P. *Inorg. Chem.* **1989**, *28*, 4650–4656.

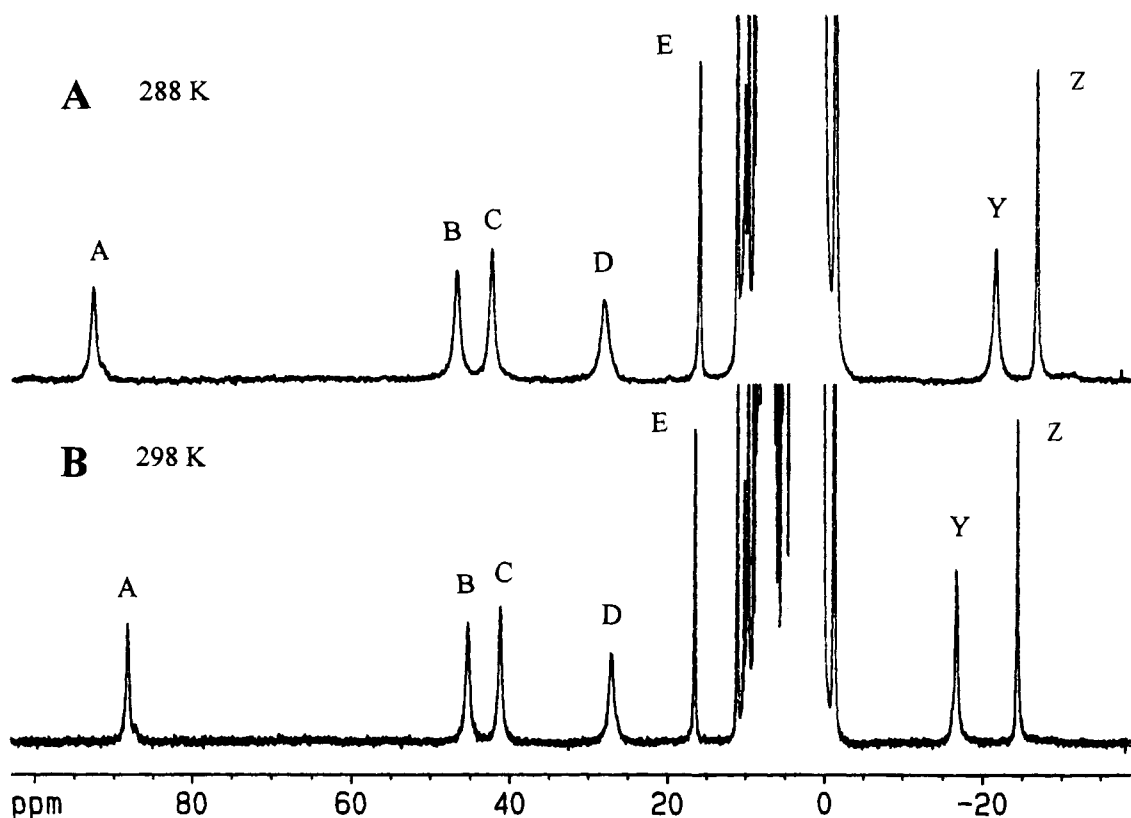


Figure 2. 600 MHz ^1H NMR spectra of oxidized HiPIP I from *E. halophila* at 288 K (A) and 298 K (B). The spectra were recorded in H_2O solutions, 50 mM phosphate buffer at pH 5.1. The assignment of labeled signals is reported in Table 1.

discriminate between first- and second-order NOEs. Furthermore, the experiments were repeated using two different values for the spectral window. In one series of 1D NOE experiments, the spectral window was maintained at 125 kHz using 8192 data points to quantitatively estimate the observed NOEs with respect to the irradiated signal. A second series of experiments was then performed using the same number of data points and a spectral window of 8.6 kHz. This provided a much higher resolution, thereby allowing a better analysis of the 1D NOEs observed in the diamagnetic region. All of the 1D NOE experiments were performed in both H_2O and D_2O solutions in order to identify the exchangeable or partially exchangeable NH signals close to the prosthetic group. T_1 values for the hyperfine shifted signals were measured using an inversion recovery sequence.³³

All data were processed on a Bruker X32 computer, using the standard software package provided by Bruker.

Results

In the ^1H NMR spectra of oxidized recombinant HiPIP I from *E. halophila*, recorded at pH 5.1, seven hyperfine shifted signals are observed between +100 and -30 ppm (Figure 2). As evident in Figure 2, all hyperfine shifts, except that of signal E, decrease as the temperature is increased from 288 to 298 K. At infinite temperature, signals Y and Z extrapolate to the far-downfield region, as does signal E. The temperature-dependent properties of these signals can be analyzed on the basis that we have developed and applied in our studies of the hyperfine coupling in other oxidized 4Fe-4S clusters. As in the case of HiPIPs from other bacterial sources,^{18,34–37} the four most downfield-shifted resonances arise from the protons of cysteines

bound to the two iron ions that are predominantly in the +2.5 valence state. The two upfield signals and the downfield signal E are assigned to protons of cysteines bound to the two iron ions in the pure or predominantly ferric states.

A NOESY experiment recorded at 288 K, shown in Figure 3, revealed the relatively strong connectivities characteristic of βCH_2 pairs between signals A and D, signals B and C, and signals Y and Z, respectively. Furthermore, connectivities were observed between signal E and three signals in the diamagnetic region, at 2.6 (F), 6.3 (G), and 8.6 (H) ppm, respectively (Figure 3). Repetition of this experiment at 292 K recorded at short irradiation times (Figure 4E, upper trace) shows that signals F and G have a strong anti-Curie temperature dependence, similar to that of signal E. The line widths of signals F and G (280 and 450 Hz, respectively), as measured from 1D NOE difference spectra and the slope of the temperature dependence of these signals, indicate that these two signals are βCH_2 protons of a cysteine bound to a predominantly ferric ion. The extent of the NOEs experienced by signals F and G from signal E and the T_1 value of the latter (Table 1) indicate that signal E is the $\text{H}\alpha$ proton of the cysteine to which signals F and G belong.

The chemical shifts and the T_1 values for the hyperfine shifted signals are summarized in Table 1.

Sequence-Specific Assignment of Oxidized, Recombinant HiPIP I from *E. halophila*. As the assignment of the reduced form of the protein is known,³⁸ the assignment of the oxidized

(33) Vold, R. L.; Waugh, J. S.; Klein, M. P.; Phelps, D. E. *J. Chem. Phys.* **1968**, *48*, 3831–3832.

(34) Bertini, I.; Capozzi, F.; Luchinat, C.; Piccioli, M.; Vicens Oliver, M. *Inorg. Chim. Acta* **1992**, *198–200*, 483–491.

(35) Bertini, I.; Capozzi, F.; Ciurli, S.; Luchinat, C.; Messori, L.; Piccioli, M. *J. Am. Chem. Soc.* **1992**, *114*, 3332–3340.

(36) Luchinat, C.; Ciurli, S. *Biol. Magn. Reson.* **1993**, *12*, 357–420.

(37) Luchinat, C.; Ciurli, S.; Capozzi, F. In *Perspectives in Coordination Chemistry*; Williams, A. F., Floriani, C., Merbach, A. E., Eds.; VCH: Basel, 1992; pp 245–270.

(38) (a) Bertini, I.; Felli, I. C.; Kastrau, D. H. W.; Luchinat, C.; Piccioli, M.; Viezzoli, M. S. *Eur. J. Biochem.* **1994**, *225*, 703–714. (b) Banci, L.; Bertini, I.; Eltis, L. D.; Felli, I. C.; Kastrau, D. H. W.; Luchinat, C.; Piccioli, M.; Pierattelli, R.; Smith, M. *Eur. J. Biochem.* **1994**, *225*, 715–725.

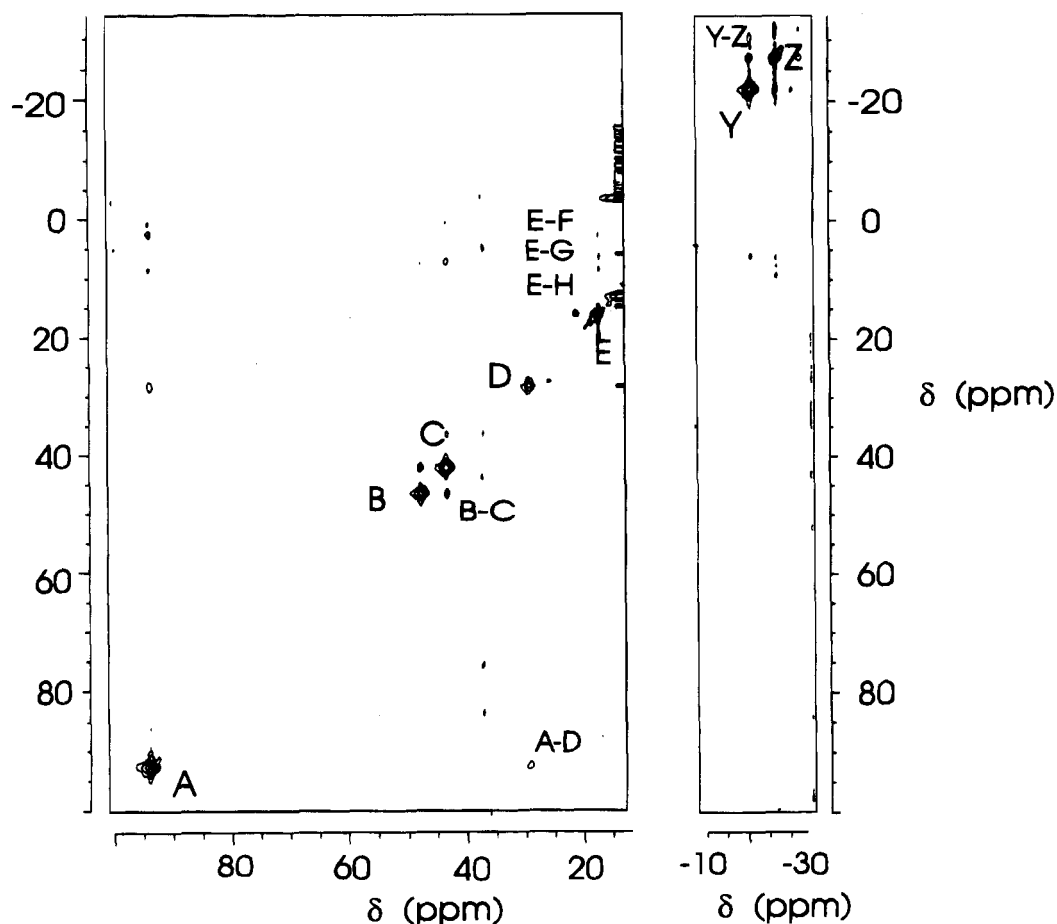


Figure 3. 600 MHz, 288 K NOESY spectrum of oxidized HiPIP I from *E. halophila*. The two panels show the downfield part of the spectrum, in which the connectivities involving signals A–H are observed, and the upfield part, where signals Y and Z are observed. The spectrum was recorded with mixing and recycle delays of 9 and 62 ms, respectively. In order to reduce the overall spectral window, the carrier frequency was placed at +36.3 ppm and an off-resonance DANTE sequence was used for water presaturation.

form might be readily performed through saturation transfer experiments, provided that the rate of electron self-exchange occurs on a suitable time scale.³⁹ In saturation transfer experiments performed on a sample containing both oxidized and reduced species, no connectivities due to electron self-exchange between the two species were observed. Therefore the assignment of the oxidized form was performed independently. The saturation transfer experiment places an upper limit of about $10^3 \text{ M}^{-1} \text{ s}^{-1}$ on the rate constant of electron self-exchange in HiPIP I from *E. halophila*. This agrees well with the rate constants of electron self-exchange that have been determined for many other HiPIPs using the same technique.²²

The sequence-specific assignment of the hyperfine shifted resonances of the oxidized protein was initiated by inspection of the 1D NOE difference spectra obtained upon saturation of each the seven hyperfine shifted signals, both in H_2O and D_2O , and by comparing the observed 1D NOE peaks with the data obtained from NOESY and TOCSY experiments performed in the +12 to –2 ppm region. The assignment of the cysteine protons, presented in Table 1, was completed by considering these data in the context of the solution structure of the reduced HiPIP,³⁸ which is expected to be very similar to that of the oxidized HiPIP. The best evidence for these assignments, obtained from the most significant NOEs depicted in Figure 4, is discussed below. While not discussed here, these assignments are completely consistent with the numerous smaller NOEs

observed for the hyperfine signals, almost all of which have now been assigned.

The upfield signals Y and Z were assigned to Cys 33 on the basis of the dipole–dipole connectivities that occur between signal Y and two signals (1 and 2 in Figure 4) of the six-membered ring of a Trp residue. The complete spin pattern of this ring is indicated by the dotted lines in the aromatic region of the TOCSY spectrum, recorded in D_2O (Figure 5A). Signals 1 and 2 correspond to two of the four resonances of this pattern. In the solution structure of the reduced form of the protein, Cys 33 $\text{H}\beta_2$ is within 3.0 Å of the $\text{H}\epsilon_3$ and $\text{H}\zeta_3$ protons of Trp 39. Thus, signal Y is assigned to Cys 33 $\text{H}\beta_2$. Irradiation of signal Z, which would be the geminal proton of signal Y, also yielded NOEs to signals 1 and 2, although to a smaller extent. More significantly, signal Z showed three NOEs with HN protons (peaks 3–5 in Figure 4), two of which (3 and 4) were also observed upon irradiation of signal Y. TOCSY spectra indicated that signal 4 is the HN proton of a long-chain residue (Figure 5B) and that signal 5 is the HN proton of a Gly residue. These data are only consistent with signal Z being Cys 33 $\text{H}\beta_1$, which in the reduced HiPIP is in close proximity to the HN of Glu 34 (signal 4), the HN of Gly 64 (signal 5), and the HN of Cys 33 (3). No cross peak could be detected in the TOCSY spectrum for signal 3 due to the cluster-induced broadening of the signal arising from the Cys 33 $\text{H}\alpha$ proton. In the reduced HiPIP, this $\text{H}\alpha$ proton is 3.2 Å from an iron ion and 2.9 Å from a sulfide ion of the cluster.

The Cys $\text{H}\alpha$ proton signal E was assigned to Cys 66 on the basis of the observed NOEs to the two signals 6 and 7, which

(39) Ernst, R. R.; Bodenhausen, G.; Wokaun, A. *Principles of Nuclear Magnetic Resonance in One and Two Dimensions*; Oxford University Press: London, 1987;

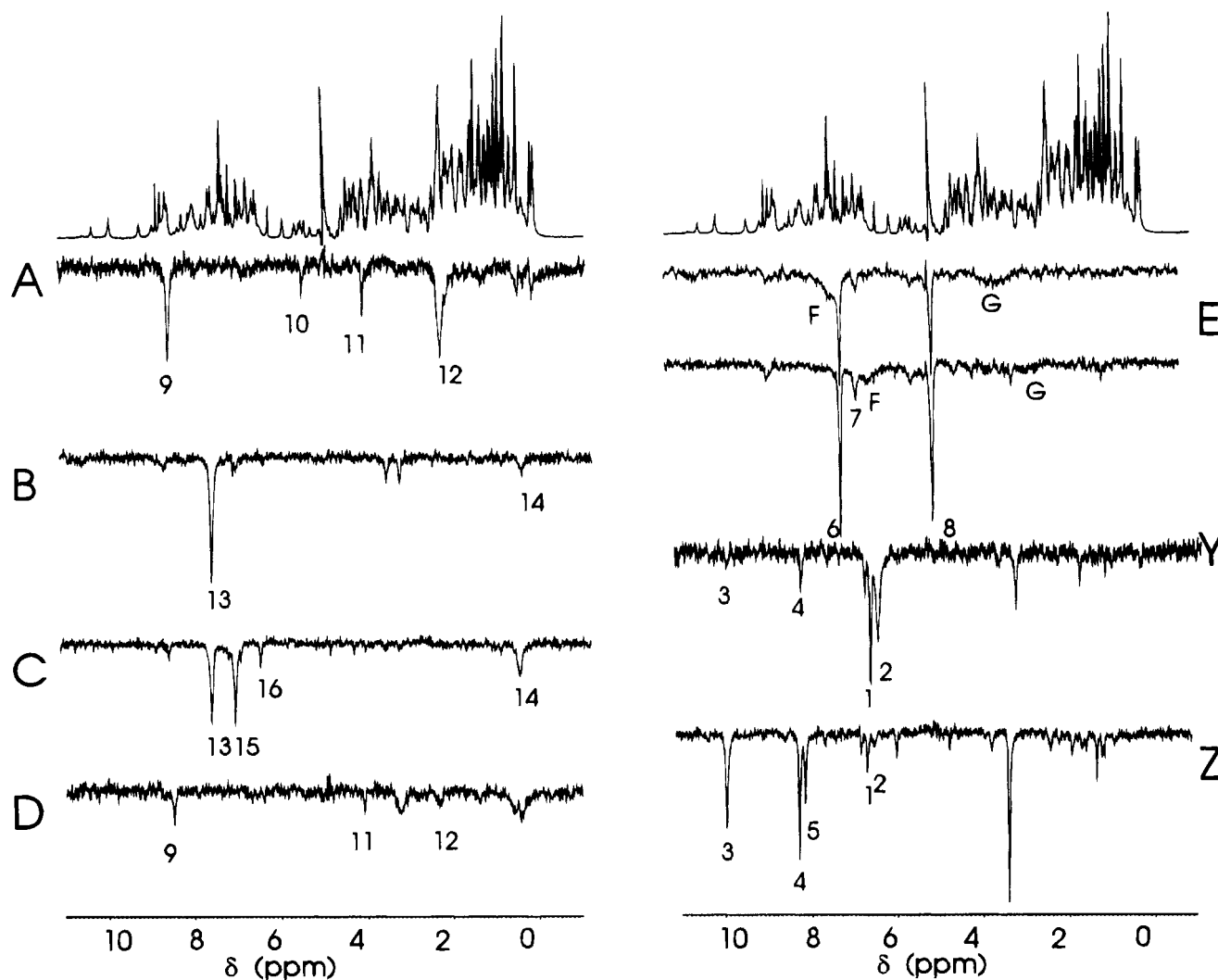


Figure 4. 600 MHz, 288 K 1D NOE difference spectra obtained upon selective saturation of the seven hyperfine shifted signals. Only the +11 to -1 ppm region is reported. The label of each trace corresponds to the label of the saturated signal. The two E traces were recorded at 292 K (upper) and 288 K (lower). The labeled NOE difference peaks are discussed in the text. The spectra were collected in D_2O solution, using a saturation time of 170 ms, except for the upper trace of E, which was recorded with a saturation time of 20 ms.

Table 1. Chemical Shifts, T_1 Values, and Line Widths of Cysteine Proton Signals in Oxidized HiPIP I from *E. halophila* at 600 MHz, 298 K, and pH 5.1 (T_1 at 281.5 K)

signal	δ (ppm)	T_1 (ms)	$\Delta\nu$ (Hz)	assignment
A	88.3	7.4	240	Cys 50 $H\beta_2$
B	45.3	4.8	320	Cys 36 $H\beta_2$
C	41.2	5.8	300	Cys 36 $H\beta_1$
D	27.1	3.6	430	Cys 50 $H\beta_1$
E	16.6	48.3	85	Cys 66 $H\alpha$
F	8.3		280 ^a	Cys 66 $H\beta_1$
G	4.1		450 ^a	Cys 66 $H\beta_2$
Y	-16.7	11.8	200	Cys 33 $H\beta_2$
Z	-24.4	34.6	100	Cys 33 $H\beta_1$

^a Measured at 292 K from 1D NOEs.

correspond to He_3 and $H\zeta_3$ of another Trp residue. Again, on the basis of the reduced HiPIP structure, Cys 66 is the only cysteine whose α proton is expected to be located within 3.6 Å of two Trp ring signals (Trp 65). The four-spin pattern of Trp 65 is indicated in Figure 5A by the dashed lines, two spins of which correspond to signals 6 and 7. The assignment of signal E to the Cys 66 $H\alpha$ proton is corroborated by its strong NOE to signal 8, which corresponds to the $H\alpha$ proton of an AMX spin system. This is consistent with the structural evidence that Cys 66 $H\alpha$ is close in space to the $H\alpha$ proton of Tyr 14. The stereospecific assignment of the $H\beta$ protons of Cys 66, whose

signals lie in the diamagnetic envelope, is based on the intensities of the H-H NOEs and the line widths of the two NOEs observed to signals F and G (280 and 450 Hz, respectively). The larger NOE to signal F as compared to signal G indicates that it is closer to Cys 66 $H\alpha$ while the narrower line width of the former suggests that it is farther from the cluster. This is perfectly consistent with the solution structure of the reduced protein when signals F and G are assigned to the $H\beta_1$ and $H\beta_2$ protons, respectively.

Irradiation of signal A yielded major NOEs to four signals (9–12 in Figure 4) which, with the exception of signal 10, were also observed upon irradiation of signal D. Signal 9 was assigned to the HN proton of Cys 50 because no spin pattern was observed in the TOCSY spectrum and because both Cys $H\beta$ protons displayed a strong dipolar connectivity to this signal. Inspection of NOESY maps revealed that signals 10 and 12 arise from the $H\alpha$ and $H\beta$ of a Phe residue. TOCSY experiments demonstrated that signal 11 is the $H\alpha$ proton of an Arg residue. The spin pattern of this Arg residue, observed partly from the amide HN proton and partly from the HN proton, is clearly discerned in Figure 5C, which depicts a portion of the TOCSY spectrum recorded in H_2O . The $H\alpha$ proton of this residue (signal 11) displayed a dipole-dipole connectivity to the HN signal 9. In the reduced HiPIP, Cys 50 is the only

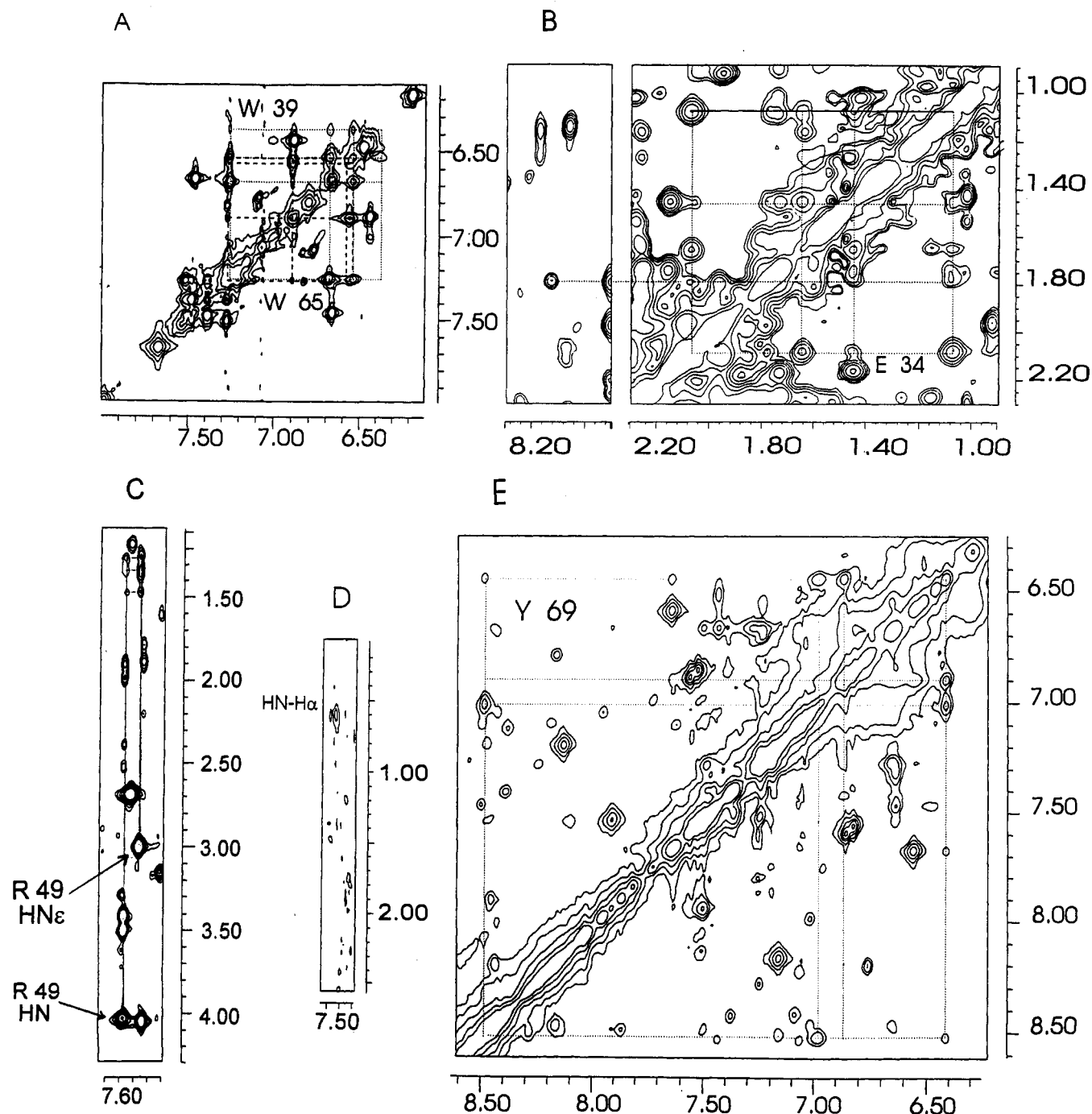


Figure 5. 600 MHz, 288 K two-dimensional spectra of oxidized HiPIP I from *E. halophila*. (A) Aromatic region of a TOCSY spectrum recorded in D_2O is reported. Two four-spin patterns, corresponding to two Trp residues (W 39 and W 65) are delineated. (B) Two portions of a TOCSY spectrum recorded in H_2O are reported. The aliphatic five-spin pattern of a Glu residue (E 34) and the HN-H α connectivity are shown. The anomalous chemical shift value of the H α proton of Glu 34 is consistent with that reported for the reduced form of the protein. (C) Spin pattern unambiguously corresponding to an Arg residue (R 49), observed in a TOCSY spectrum, recorded in H_2O . It is observed that both HN (left column, dotted line) and HN ϵ (right column, dotted line) give rise to connectivities with the aliphatic protons of this long-chain residue. (D) Region of a TOCSY spectrum, recorded in H_2O solution with 14 ms of spin lock time, in which the connectivity between HN and H α proton of Cys 36 is observed. (E) Aromatic region of a NOESY spectrum, recorded in H_2O , in which the pattern of the intra-residue NOEs of a Tyr residue (Y 69) is observed.

cysteine that is close to an arginine (Arg 49) and Cys 50 H β_2 is the only Cys proton that is within 3.0 Å of a Phe H β proton (Phe 55). The described connectivities are completely consistent with signal A being Cys 50 H β_2 . Signal D, assigned to Cys 50 H β_1 , yielded no major NOEs other than those discussed.

With respect to the final cysteine, Cys 36, signals B and C both displayed strong NOEs to two signals (13 and 14 in Figure 4). Signal 13 gave no TOCSY pattern when such experiments were performed with a spin lock time of 45 ms. Repetition of the TOCSY experiment with a 14 ms spin lock time enabled

the observation of a weak cross peak with signal 14 (Figure 5D). Such connectivity were also detected in the NOESY experiment when short mixing times were used. This permits the assignment of signals 13 and 14 to the HN and H α protons of Cys 36. Evidence for the sequence-specific and the stereospecific assignment of signals B and C is provided by the strong NOEs of the latter on two signals, labeled 15 and 16 in Figure 4. Signals 15 and 16 belong to a pattern of a Tyr ring, indicated by dotted lines in the aromatic region of the NOESY spectrum, recorded in H_2O , shown in Figure 5E and confirmed

by TOCSY experiments. The four resonances observed in this spectrum arise from the exchangeable signal of the hydroxyl group of the Tyr, signals of two He protons, and a signal arising from Hd protons, whose signals coalesce. Two of these four signals, namely one of the He and one of the Hd, correspond to signals 15 and 16. In the reduced HiPIP, Cys 36 is the only cysteine that is close in space to a tyrosine ring (Tyr 69) and, indeed, Cys 36 H β_1 is within 3.0 Å of both Hd $_1$ and He $_1$ of Tyr 69, thus enabling the assignment of signal C to Cys 36 H β_1 and, by default, that of signal B to Cys 36 H β_2 .

In ending this section, we note that the sequence-specific assignment of the signals of the oxidized form of recombinant HiPIP I of *E. halophila* follows an NOE pattern similar to that encountered in the native HiPIP II of the same bacterium.¹⁸ The various NOE difference spectra of the two proteins are comparable in terms of both the shifts and the intensities of the observed NOE peaks.

Discussion

The oxidized recombinant HiPIP I from *E. halophila* has a ¹H NMR spectrum that is unique in comparison to those of the other characterized HiPIPs.^{16,19–21,40–42} The spectrum, which is essentially identical to that of the WT protein,¹⁶ except for the better resolution obtained at 600 MHz, has only seven hyperfine shifted signals, rather than eight or nine as observed in the spectra of other HiPIPs. The “missing” signals, assigned to the β CH $_2$ protons of Cys 66 (signals F and G, Table 1), were located in the diamagnetic region of the spectrum through experiments designed to detect connectivities between fast-relaxing signals. The hyperfine shifts of these protons are appreciably smaller than those of the corresponding protons in other HiPIPs, even though the hyperfine shifts experienced by the β CH $_2$ protons of each of the other cysteines (Cys 33, 36, and 50) are similar in magnitude to those of the corresponding protons in the other HiPIPs investigated to date.^{18,21–23,34,35} Furthermore, this peculiarity, in which the hyperfine coupling with the corresponding iron ion appears to be quenched, is associated with the properties of the oxidized cluster as the hyperfine shifts of the same cysteine β CH $_2$ protons in the reduced protein (11.06 and 6.00 ppm³⁸) are very similar to those observed for the other investigated HiPIPs.²¹

Far from being an anomalous case, however, the NMR spectrum of oxidized HiPIP I from *E. halophila* strengthens and extends the theoretical model we have developed to rationalize the NMR properties of other HiPIPs.^{19,43} This system constitutes a nice example of an intermediate situation between HiPIP II from *E. halophila* (Figure 1B) and the other HiPIPs (Figure 1C), in which the iron ion bound to Cys 66 in *E. halophila* HiPIP I effectively possesses no hyperfine coupling around room temperature. This conclusion is validated by the strong temperature dependence of the two β CH $_2$ signals of Cys 66, which is similar to the temperature dependence of these signals in other HiPIPs. The slope of this dependence indicates that these signals could travel across the entire diamagnetic region of the spectrum (ca. 10 ppm) over 50 K; *i.e.*, they would be predicted to disappear into the diamagnetic region between 255 and 275 K and to reappear on the downfield side above 305–325 K.

The hyperfine shifted signals have been sequence specifically assigned to the cysteine β CH $_2$ protons in seven HiPIPs,^{18,21–23,34,35}

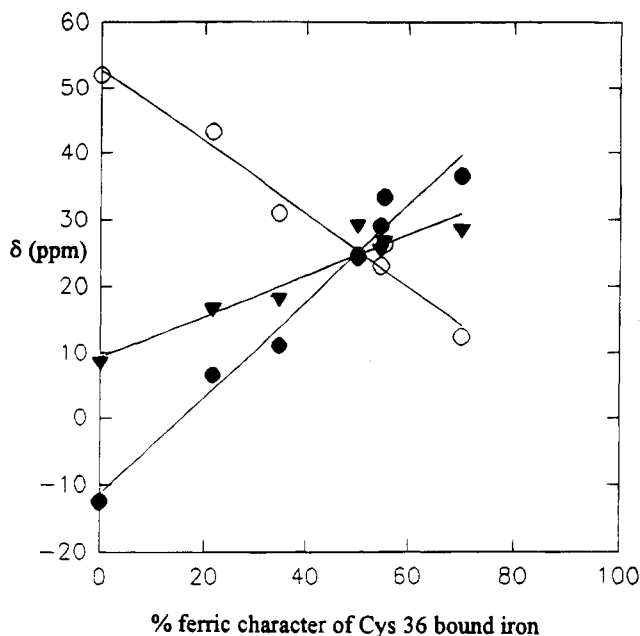


Figure 6. Averaged hyperfine shifts of the β CH $_2$ protons of Cys 36 (O) and Cys 66 (●) and hyperfine shifts of the α CH proton of Cys 66 (▼) versus the percentage of the electronic configuration represented by Figure 1D. The latter was estimated by taking the chemical shift values of Cys 36 and Cys 66 β CH $_2$ in HiPIP II from *E. halophila* as the limiting shift values of purely mixed-valence and purely ferric pairs, respectively. For each investigated HiPIP, the averaged shifts of Cys 36 and Cys 66 were then compared to the values of the purely ferric and a purely mixed-valence pair, to obtain the percentage of ferric character of the iron bound to Cys 36 and of mixed-valence character of that bound to Cys 66. The average of the two values obtained as above is reported on the abscissa for each HiPIP. Thus, the abscissa reports the percentage ferric character of the iron bound to Cys 36, the percentage mixed-valence character of the iron bound to Cys 66, and, by extension, the percentage of the cluster in the electronic configuration depicted on the right of the equilibrium Figure 1A. The data (from left to right) refer to the HiPIPs from the following organisms: *E. halophila* (iso II), *E. halophila* (iso I, present work), *R. globiformis*, *E. vacuolata* (iso I), *E. vacuolata* (iso II), *C. vinosum*, *R. gelatinosus*.

including the current system. Examination of the variation of these hyperfine shift values in these proteins reveals that it is the shifts of the Cys 36 and Cys 66 (recombinant HiPIP I from *E. halophila* numbering) β CH $_2$ protons that undergo the greatest variation. According to the equilibrium model of the electronic structure of the cluster, it is the iron ions bound to these residues that can exist in either the +2.5 or +3 valence state (II and IV of Figure 1A). Indeed, we believe that these hyperfine shifts can be used to estimate the position of the equilibrium in a given HiPIP cluster. As described above, it can be assumed that HiPIP II from *E. halophila* represents an extreme situation in which the cluster exists in one electronic state. Thus, *both* cysteines coordinated to the ferric irons (Cys 33 and 66) reflect the positive (S_z) value of each of the corresponding irons. The average hyperfine shifts experienced by the β CH $_2$ protons of Cys 66 in the latter system (ca. -15 ppm) are taken as representative of a 100% ferric situation. Similarly, the average hyperfine shift of the β CH $_2$ protons of Cys 36 (ca. 50 ppm) is assumed to represent the shifts of β CH $_2$ protons of a cysteine bound to a 100% mixed-valence iron. In the seven HiPIPs under consideration, the β CH $_2$ protons of Cys 33 and 50 experience average shifts of 68 ± 8 and -26 ± 9 ppm, respectively. For each HiPIP, the percentage of ferric versus mixed-valence character of each of the irons bound to Cys 36 and 66 may be estimated by comparing the hyperfine shifts of the CH $_2$ protons of these residues in the HiPIP to those in *E. halophila* HiPIP II.

(40) Krishnamoorthi, R.; Cusanovich, M. A.; Meyer, T. E.; Przysiecki, C. T. *Eur. J. Biochem.* **1989**, *181*, 81–85.

(41) Nettlesheim, D. G.; Meyer, T. E.; Feinberg, B. A.; Otvos, J. D. *J. Biol. Chem.* **1983**, *258*, 8235–8239.

(42) Cowan, J. A.; Sola, M. *Biochemistry* **1990**, *29*, 5633.

(43) Banci, L.; Bertini, I.; Ferretti, S.; Luchinat, C.; Piccioli, M. *J. Mol. Struct.* **1993**, *292*, 207–220.

A plot of the proton average hyperfine shifts of residues 36 and 66 as a function of the estimated percentage of ferric or mixed-valence character of the iron bound to them is shown in Figure 6. While this figure is empirical and was derived without an independent assessment of the electronic structure of the cluster, it is nevertheless instructive. First, the good overall correlation graphically depicts that the apparently negligible hyperfine shift of the Cys 66 βCH_2 protons in *E. halophila* HiPIP I is entirely consistent with our current view of the electronic structure of HiPIP clusters. The magnitude of this shift is a manifestation of the proportion (about 80:20) of ferric and mixed-valence character of the iron bound to that residue. Second, the shifts of both Cys 36 and Cys 66 correlate reasonably well with the estimated percentage. Third, among the seven characterized HiPIPs, the shifts of the βCH_2 protons of the present system are those that are closest in value to the corresponding shifts in the isoprotein HiPIP II from the same bacterial source. This is consistent with the sequences similarities in these seven proteins, though we note that there is no obvious relationship between the electronic structure and reduction potential of the clusters. Fourth, as is apparent from the right-hand side of Figure 6, a system has yet to be identified in which the electronic structure of the irons coordinated to Cys 36 and Cys 66 is completely reversed with respect to the *E. halophila* iso-II case.¹⁸ The system which is most different from *E. halophila* iso-II is *R. gelatinosus*,³⁴ for which the ferric:mixed-valence proportion reaches approximately 70%. From the plot of Figure 6 it is thus possible to have a roughly quantitative estimation of the percentage of the equilibrium between the two possible electronic distributions for all the investigated HiPIPs at room temperature.

The shift of signal E, arising from the $\text{H}\alpha$ proton of Cys 66, is also reported in Figure 6. This signal is the only $\text{H}\alpha$ proton found outside the diamagnetic region of the spectrum of any

HiPIP. Consistent with the behavior of the βCH_2 proton shifts, the shift of this proton also appears to be a function of the electronic structure of the cluster, albeit to a lesser extent. However, the shift of signal E is clearly influenced by another factor. This can be appreciated by considering the hyperfine shifts of the Cys 66 protons in *E. halophila* HiPIP II: the βCH_2 protons are shifted considerably upfield, while the H proton is still downfield, although in the diamagnetic region. All things being equal, a reversal in sign of the $\langle S_z \rangle$ of the iron bound to Cys 66 should result in a reversal in sign of the hyperfine shifts of all Cys 66 protons. The observed behavior of the $\text{H}\alpha$ proton of Cys 66 can be reconciled with this expectation by postulating the existence of a contribution of unknown origin to its hyperfine shift. The magnitude of this contribution is approximately 13 ppm downfield and is present in all of the HiPIPs studied to date.

In summary, the sequence-specific assignment of cysteine protons of the oxidized recombinant HiPIP I from *E. halophila* reported here is of particular interest due to the unique chemical shift values of the Cys 36 and Cys 66 protons in this protein. The proportion of the two electronic distributions in this cluster was estimated to be 20:80, and thus the equilibrium lies between that of *E. halophila* HiPIP II (0:100) and the other HiPIPs, most of which are around 50:50. The current data thus strongly corroborate the equilibrium model for the electronic structure of the oxidized HiPIP cluster and allow the proposition of an empirical relationship between hyperfine shifts and position of this equilibrium.

Acknowledgment. This research was partly financed by the Progetto Finalizzato Biotecnologie, Consiglio Nazionale delle Ricerche (CNR), and by the Comitato Scienze Agrarie, CNR.

IC950003Q